HHS Public Access

Author manuscript

Kidney Int. Author manuscript; available in PMC 2013 July 01.

Published in final edited form as:

Kidney Int. 2013 January ; 83(1): 84–92. doi:10.1038/ki.2012.336.

Tubular expression of heat shock protein 27 inhibits fibrogenesis in obstructive nephropathy

Aparna Vidyasagar, PhD[1,*], **Shannon Reese, BS**[1,*], **Omeed Hafez, BBA**[1], **Ling-Jin Huang, MD**[1], **William Swain, PhD**[1], **Lynn Jacobson, BS**[1], **Jose Torrealba, MD**[2], **Pierre-Emmanuel Chammas, MD**[1], **Nancy A. Wilson, PhD**[1], and **Arjang Djamali, MD**[1]

[1]Divisions of Nephrology University of Wisconsin School of Medicine and Public Health, Madison, WI

[2]Divisions of Pathology and Laboratory Medicine University of Wisconsin School of Medicine and Public Health, Madison, WI

Abstract

Morphological changes that occur during kidney injury involve actin skeleton remodeling. Here we tested whether heat shock protein 27 (HSP27), a small stress response protein involved in cytoskeletal remodeling, protects the kidney from tubulointerstitial fibrosis in obstructive nephropathy. Tubular cell HSP27 immunostaining was significantly increased in human kidneys with ureteropelvic junction obstruction; supporting the clinical relevance of our studies. To develop an animal model for mechanistic studies we generated transgenic mice that specifically overexpress human HSP27 in renal tubules, under the kidney androgen-regulated protein promoter, and determined the effects of HSP27 overexpression on epithelial-to-mesenchymal transition and tubulointerstitial fibrosis following unilateral ureteral obstruction. This was associated with decreased fibrogenesis as evidenced by significant declines in phosphorylated p38MAPK, collagen III, α-smooth muscle actin, 4-hydroxynonenal, and reduced trichrome staining following obstruction. Notably, E-cadherin and β-catenin remained at the cell membrane of tubular cells in transgenic mice with an obstructed ureter. Monocyte/macrophage infiltration, however, was not significantly affected in these transgenic mice. Thus, tubular HSP27 inhibits fibrogenesis in obstructive nephropathy. Further studies are needed to determine pathways regulating the interactions between HSP27 and the E-cadherin-β-catenin complex.

Introduction

Renal tubulointerstitial fibrosis or IFTA (interstitial fibrosis and tubular atrophy) is the point of pathological commonality for native and transplant kidney disease[1]. Fibrotic damage is associated with the presence of interstitial fibroblasts and myofibroblasts. A distinguishing

Corresponding Author Dr. Arjang Djamali 5142 MFCB 1685 Highland Ave. Madison, WI 53705 Telephone: 608-265-7593 FAX: 608-263-6743 axd@medicine.wisc.edu.

*These authors contributed equally to the work

Disclosure The authors declare no conflict of interest.

characteristic of myofibroblasts is their expression of α-smooth muscle actin (α-SMA). These cells are also responsible for the deposition of extracellular matrix proteins such as collagens I, III, IV and fibronectin. Tubular atrophy entails the loss of tubular epithelial cells through apoptotic and necrotic pathways as well as through transition to a mesenchymal phenotype. A better understanding of the cellular and molecular mechanisms involved in IFTA would result in the development of preventive and therapeutic interventions that improve long-term outcomes in patients with native and transplant kidney disease.

Epithelial-to-mesenchymal transition or EMT is an important profibrotic process and a surrogate marker of native and transplant kidney fibrosis[2–5]. TGF-β1 is the primary cytokine that initiates and maintains EMT by activating signaling pathways and transcriptional regulators such as Smad 2/3 molecules. During EMT, tubular epithelial cells are transformed into myofibroblasts through processes involving loss of cell-cell adhesion molecules (e.g. E-cadherin) and *de novo* expression of mesenchymal markers (e.g. α-SMA). These events are followed by tubular basement membrane disruption, cell migration and fibroblast invasion of the interstitium with production of fibrotic molecules including collagen and fibronectin. Iwano et al demonstrated that up to one third of interstitial fibroblasts could originate from the epithelium during renal injury; suggestive of EMT *in vivo*[6]. Another recent fate mapping study by Humphreys et al suggests that pericytes may be another important source of interstitial myofibroblasts[7]. Although the exact contribution of EMT to renal fibrosis remains unknown, this pathway has been extensively studied as a reversible injury process and a surrogate marker of native and transplant kidney fibrosis[2, 3, 5].

Heat Shock Protein 27 (HSP27) is a small molecular weight stress response protein originally characterized as a molecular chaperone induced by heat shock[8]. Over time, HSP27 has emerged as a dynamic protein with diverse roles in regulation of actin cytoskeletal remodeling[9, 10] apoptosis[11, 12] and oxidative stress[9, 13, 14]. Renal fibrogenesis and EMT include several processes that may involve HSP27[10, 15]. For example, HSP27 is activated *via* phosphorylation by p38MAPK signaling, an important injury pathway in inflammation and oxidative stress[16, 17]. Similarly, reactive oxygen species (ROS), known inducers of HSP27, play an important role in the pathogenesis of EMT and IFTA[16, 17]. In addition, the morphological changes that occur during EMT entail actin skeleton remodeling[2–5], suggesting that HSP27 regulates actin filament dynamics and actin-cadherin junction interactions during this process.

Previous studies from our laboratory have examined the role of tubular HSP27 in experimental models of transplant and native kidney disease[18, 19]. These studies demonstrated that cortical HSP27 was upregulated in response to allograft injury, suggestive of a local stress-response to chronic rejection[19]. Similarly, we observed that tubular HSP27 was upregulated in the *in vitro* model of TGF-β1-induced EMT and during experimental obstructive nephropathy[16]. In these studies, the overexpression of human HSP27 (Hu27) in rat tubular epithelial cells preserved E-cadherin protein levels during EMT leading us to hypothesize that HSP27 plays an active and protective role during renal fibrogenesis[18, 19]. In the current manuscript, we hypothesize that elevated tubular HSP27 reduces fibrogenesis. We test our hypothesis *in vitro* and *in vivo*, using human samples and an animal model of

obstructive nephropathy, a condition that is an important cause of end-stage renal disease (ESRD) in the pediatric population[16].

Results

HSP27 was increased in tubules of pediatric kidneys with congenital ureteropelvic junction (UPJ) obstruction

To determine the relevance of our studies in the clinical setting, we examined HSP27 expression in 5 obstructed and 5 control human and mouse kidneys. Controls included pre-implantation biopsies from deceased donor kidneys prior to transplantation in humans, and baseline unobstructed kidneys in mice. Using the Nuance digital analysis software system, we found that HSP27 was significantly increased in tubules of obstructed kidneys (Figure 1).

Development of HSP27 transgenic mice

We developed HSP27 transgenic mice that overexpress human HSP27 in the proximal tubule, using the KAP2 promoter and human angiotensinogen (hAGT) enhancer complex as described previously[20]. The presence of the KAP2-HSP27 transgene was first determined by PCR of genomic DNA from tail snips (Figure 2). The transgene was evidenced by a distinct band migrating between 0.5 and 0.7 kb (Figure 2B). KAP2-HSP27 transgenic male mice expressed the transgene in the cortex of the kidney. Next, we examined expression of the KAP2-HSP27 gene by imaging eGFP fluorescence using the Caliper IVIS Spectrum optical imaging system (Figure 2C). Spectral analysis indicated 465 nm excitation and 520 nm emission wavelengths were optimal for detection of eGFP. Transgenic animals showed significantly greater fluorescence in the kidney but not the heart compared to wild-type animals, consistent with the specificity of the KAP2 promoter and hAGT enhancer[20].

HSP27 upregulation was greater in KAP2-HSP27 transgenic mice after UUO

To determine whether HSP27 was differentially upregulated by UUO in the transgenic mice, we performed western blot and immunohistochemical analyses in obstructed kidneys of transgenic and wild type littermates (Figure 3). Animals were sacrificed at 7 and 14 days post UUO for time-course analyses. Total and phosphorylated HSP27 levels were significantly increased in transgenic mice at both days 7 and 14 (Figure 3B). We analyzed the ratio of phosphorylated-to-total HSP27 in wild type and transgenic mice at baseline, 7 days and 14 days and found that the ratio remained stable in wild type mice (1.75±0.55), while it decreased in transgenic animals (1.25±0.25 to 0.85±0.55). These differences were not statistically significant. The remaining studies focused on the 14-day time point because we observed no significant difference in HSP27 expression between days 7 and 14.

HSP27 overexpression was associated with decreased fibrogenesis

To determine whether HSP27 prevents obstruction-induced fibrogenesis we examined the differences in trichrome staining in transgenic and wild type kidneys at baseline and 14 days. Red and blue areas were measured for 10 non-overlapping fields from each group (Figure 4 A and B). Mann-Whitney analysis showed that trichrome blue staining was significantly ($p<0.01$) reduced in the transgenic obstructed mice as compared to wild-type

mice (Figure 4B). Trichrome staining was minimal at baseline and not statistically significant between the two groups (bar graph not shown). We confirmed these studies by immunoblot analyses of fibrosis (collagen III and α-SMA), oxidative stress (4-Hydroxynonenal or HNE) and proinflammatory signaling (p38MAPK) (Figure 5). At baseline, phosphorylated and total HSP27 levels were greater while α-SMA was lower in transgenic mice. Following obstruction, we observed that activated (phosphorylated) p38MAPK, collagen III, α-SMA and HNE were significantly decreased in transgenic kidneys. Total p38MAPK levels remained unchanged. These data suggested that the upregulation of HSP27 was involved in the inhibition of oxidative stress and fibrosis in obstructive nephropathy. Because oxidative stress and inflammation are closely related and monocyte/macrophages play a key role in UUO, we compared the number of interstitial monocyte/macrophages per high power field (HP) in transgenic and wild type mice at baseline and after UUO. While no cortical staining was noted in either group at baseline, we found a non-statistically significant increase in kidney infiltrating cells in transgenic mice ($p=0.135$, Figure 4-C), suggesting that the antifibrotic effects of HSP27 in UUO may be independent of monocyte/macrophages.

HSP27 overexpression was associated with preservation of E-cadherin and β-catenin at the cell membrane

To specifically examine the effects of HSP27 overexpression on E-cadherin and β-catenin levels and localization, we performed immunoblot and immunofluorescence studies in unobstructed baseline and obstructed kidney samples. Western blot analyses showed no significant differences in E-cadherin or β-catenin levels between obstructed transgenic and wild type mice (Figures 6B and 6C). However, immunofluorescence studies demonstrated differences in the localization of E-cadherin and β-catenin between transgenic and wild type mice at the basolateral cell membrane or the cytoplasm (Figure 6A). Tubular epithelial cells in wild type mice showed re-distribution of E-cadherin and β-catenin from the membrane-associated cell-junction regions to the cytoplasm consistent with our previous findings[18]. In contrast, tubular cells from KAP2-HSP27 transgenic mice retained E-cadherin at the basolateral membranes. Quantitative scoring of the frequency of cytoplasmic E-cadherin confirmed this result. Wild-type mice had scores of 12.8 and 11.5 per HPF in the unobstructed and obstructed kidneys, respectively, whereas the scores for HSP27 overexpressing transgenic mice were 4.4 and 4.5 per HPF for unobstructed and obstructed kidneys, respectively. These differences in tubular cytoplasmic E-cadherin were significant ($p<0.05$) for both unobstructed and obstructed kidneys, and indicate that HSP27 overexpression preserved E-cadherin at the cell membrane.

Discussion

Studies presented in this manuscript indicate that HSP27 may play a protective role in the pathogenesis of obstructive nephropathy. We showed that tubular HSP27 is upregulated during clinical obstructive nephropathy and that its overexpression in transgenic mice is associated with reduced fibrosis and oxidative stress. Furthermore, animal studies using transgenic mice that specifically overexpress HSP27 in renal tubules indicated that E-cadherin and β-catenin were preserved at the cell membrane despite obstruction. The

consistency of findings indicates cohesive relevance of the experimental models toward understanding the molecular processes involved in obstructive renal injury, and in the progression of pathology to tubulointerstitial fibrosis.

The transgenic mice showed significantly higher HSP27 levels relative to wild type controls before and after obstruction. Since the kidney androgen protein promoter upregulates the expression of associated genes in the presence of androgens, HSP27 was upregulated in adult transgenic (and not the wild type) male mice. We noted a significant decrease in lipid peroxidation (HNE) and phosphorylated p38MAPK in obstructed transgenic kidneys, suggesting that some of the antifibrotic effects of HSP27 may be a result of its antioxidant and anti-inflammatory properties[9, 14, 21, 22]. Since inflammation is an important cause of oxidative stress, it is possible that HSP27 overexpression inhibited p38MAPK *via* negative feedback and subsequently, prevented oxidative stress. However, more direct effects of HSP27 on oxidative stress are also possible, including upregulation of intracellular reduced glutathione[22]. Although our study did not examine the specific subpopulations of macrophages, overall monocyte/macrophage infiltration of the kidneys was not significantly different between transgenic and wild type mice, suggesting that the antifibrotic effects of HSP27 might be independent of these cells.

Like most biological processes, the stress response by HSP27 may depend on the type of injury and the specific cell types affected. For example, Chen et al found that kidney injury after ischemia-reperfusion was exacerbated by HSP27 overexpression[23]. The authors showed that the severity of injury resulted from increased inflammation, possibly due to HSP27. However, in these studies, HSP27 overexpression was systemic and not kidney specific. Conversely, Kim et al reported that the delivery of HSP27 to the kidney by *in vivo* injections of a recombinant lentivirus reduced ischemia-reperfusion injury in mice[24]. Although more specific, this delivery method is limited by the efficacy of the transfection procedure, the off-target effects of the protein and its half life. Stetler et al recently demonstrated a dose-response for the level of protection observed in HSP27 transgenic mice undergoing ischemic brain injury[25, 26]. Consistent with our findings, the investigators found that low and high-expressing HSP27 transgenic mice exhibited reduced infarct volume relative to the wild-type progenitor strain, but that the high-expressing lines showed a significantly greater reduction than the low-expressing lines.

Membrane localization of E-cadherin and β-catenin is consistent with their presence at the adherens junction. β-catenin binds to the cytoplasmic tail of E-cadherin in adherens junctions where the two proteins associate with α-catenin in dynamic association with F-actin filaments[2729]. Our finding that HSP27 maintained the level and membrane association of E-cadherin and β-catenin agrees with previous reports from our group[18] and others[30, 31], indicating a role for HSP27 in regulating the cytoskeleton. Fanelli *et al* reported co-immunoprecipitation of HSP27 and β-catenin in clinical breast cancer samples indicating possible direct interaction between the two proteins[32].

In conclusion, our studies indicate that specific HSP27 overexpression in renal tubular epithelial cells is associated with reduced oxidative stress and fibrogenesis, together with stabilization of the E-cadherin/β-catenin complex at the cell membrane. Further studies are

needed to determine the cellular and molecular pathways that regulate HSP27 interactions with membrane bound complex *in vitro* and in obstructive nephropathy.

Methods

Acquisition of human tissue samples

Paraffin embedded kidney sections were provided by the Department of Pathology at the University of Wisconsin-Madison. The Institutional Review Board (IRB) approved research use of the samples. Obstructed samples were prepared from kidneys that were removed due to ureteropelvic junction (UPJ) obstruction (n=5). Control samples were prepared from pre-implantation deceased donor kidney transplant biopsies (n=5).

Development of KAP2-HSP27 transgenic mouse

The KAP2-HSP27 transgenic mouse was designed and generated at the University of Wisconsin Biotechnology Center Transgenic Animal Facility. Full-length human HSP27 cDNA (provided by Dr. Jacques Landry, Laval University, Quebec, Canada) and an internal ribosome entry site (IRES)-enhanced green fluorescent protein (eGFP) cassette (provided by Dr. William Sugden, University of Wisconsin, Madison, WI) were inserted into the Not I site of the pKAP2 vector[20] (provided by Dr. Curt Sigmund, University of Iowa, Iowa City, IA) which utilizes the Kidney Androgen promoter and a portion of the hAGT gene including an hAGT enhancer and polyadenylation region. The transgene was isolated by digestion with SpeI and NdeI, separated from the vector fragment by gel electrophoresis, extracted from agarose and purified using the QIAEX II Gel extraction Kit (cat. no. 20021, Qiagen, CA). The purified transgene fragment was microinjected into the pronuclei of fertilized FVB ova. Injected embryos were implanted in pseudopregnant female recipients. Pups were born 19–20 days after implantation. PCR genotyping identified one male and one female founder pups that were positive for the transgene. Upon maturity these founders were bred with wild-type FVB mating partners. The resulting F1 progeny were analyzed for the presence of the transgene by PCR genotyping of tail snips. Forward and reverse primers for the KAP2-HSP27 transgene were generated by the UWBC with the following sequences: KAP2 Forward (CTG GCC ATT AGA GGG TAA) and HSP27 Reverse (AGA TGT AGC CAT GCT CGT). Founder genomic DNA and KAP2-HSP27 plasmid DNA served as positive controls, water and wild type FVB genomic DNA served as negative controls. All PCR amplification was done using an Applied Biosystems Veriti thermocycler. The amplified KAP2-HSP27 PCR product migrated between 0.5 and 0.7 kb upon agarose gel electrophoresis. Once transgenic and wild-type littermates were identified, the wild-type littermates served as experimental controls. Only post pubescent (older than 4 weeks) male mice were used for experiments in order to maintain constitutive testosterone production and expression of the testosterone-dependent KAP2-HSP27 transgene.

Unilateral Ureteral Obstruction in mice

Mice were housed in the animal care facility at the William Middleton Veterans Affairs (VA) Hospital, Madison, WI. Procedures were performed in accordance with the Animal Care Policies at the VA Hospital and the University of Wisconsin-Madison. The surgery was performed as previously described[18]. Briefly, mice were anesthetized with 1–3%

isoflurane and a 1cm midline incision was made in the abdomen. The left ureter was exposed by blunt dissection, ligated at two points using 6–0 silk suture. The abdominal muscle incision and skin incision were closed separately using 6–0 silk suture. Mice were monitored after surgery until recovered, and were observed daily thereafter. Mice were sacrificed at 7 and 14 days after UUO and both kidneys were removed. The excised kidneys were cut in half laterally; one half was snap frozen in liquid nitrogen for protein extraction, and the other half was fixed in 10% buffered formalin for microscopy.

Caliper IVIS Spectrum Optical Imaging System

The Caliper IVIS Spectrum imaging system at the UW Small Animal Imaging Facility was used to detect fluorescence under trans, epi or combination illumination at multiple excitation and emission wavelengths. We used this method to confirm the presence of eGFP in post-pubescent transgenic male mouse kidneys. Freshly excised kidneys were cut in half laterally for imaging. The excitation and emission wavelengths for pure eGFP are 488 and 520 nm, respectively. A set of 10 wavelength combinations was used to cover a range of excitation (430–500 nm) and emission values (500–580 nm). The wavelengths for optimal excitation and emission in kidney were determined to be 465 and 520 nm, respectively, using epi illumination.

Immunohistochemical, immunofluorescence and trichrome staining

5 μm sections were cut from formalin-fixed, paraffin-embedded kidneys. Slides were deparaffinized in xylene and rehydrated through a graded ethanol series to H_2O. Antigen retrieval was performed at 25 psi for 2 min in 10mM citrate solution (pH= 6.0) for HSP27, and in 1 mM EDTA solution (pH= 8.0) for E-cadherin, β-catenin and monocyte/macrophages. Nonspecific background staining was blocked using 10% BSA in PBS for 1 hour. Primary staining for total HSP27 (Abcam, CA, cat. no. ab8600 diluted 1:200) and human HSP27 (Enzo, PA, cat. no. SPA-800D diluted 1:200) was done at room temperature for 1 hour then washed and incubated with 3% hydrogen peroxide for 10 minutes. The MACH 2 Rabbit HRP polymer detection system (Biocare Medical, CA, cat. no. RHRP520 MM) and DAB (Vector Labs, CA, cat. no. SK-4100) were used to develop the HRP reactions. Cover slips were secured using Cytoseal 60 mounting media. Primary antibody incubations for E-cadherin (BD Biosciences, MD, cat. no. 610153 diluted 1:100), β-catenin (BD Biosciences, MD, cat. no. 610153 diluted 1:100) and monocyte/macrophages (Abcam, cat. no. Ab59697, diluted 1/50) were done at 4°C overnight. Prior to primary staining, β-catenin sections were permeabilized with 0.3% Triton-X in PBS at room temperature for 10 mins. Anti-mouse Alexa 594 secondary antibody (Molecular Probes, CA, cat. no. A1105 diluted 1:1000) was used at room temperature for 40 min to vizualize E-cadherin, β-catenin and monocyte/macrophages. Coverslips were secured using ProLong Gold Antifade reagent with DAPI (Invitrogen, CA, cat. no. P36931). For trichrome staining, slides were placed in Bouin's Fixative and allowed to mordant for 1 hour at 56°C, washed in tap water for 5 minutes followed by a 7 minute stain in Wiegert's Hematoxylin then washed for 3 minutes. The slides were stained in trichrome aniline blue (American MasterTech, Lodi, CA, cat # STOSTB) for 5 minutes followed by a tap water wash. Slides were dehydrated through absolute alcohol and cleared in xylene. Coverslips were secured using Cytoseal 60 mounting media. For monocyte/macrophages, the slides were quantitatively analyzed under light

microscopy. For each kidney, 10 nonoverlapping 40× fields were randomly analyzed in the cortex. Only the spots stained in deep brown were counted. Results were reported as a bar graph representing the average number of monocyte/macrophages per high power field (HPF).

For-E cadherin-β-catenin distribution analyses, slides were viewed on a Nikon Eclipse E600 microscope with an Olympus DP70 camera. The distribution of E-cadherin in the cytoplasm of renal tubules was quantified by counting the number of tubules containing purely cytoplasmic E-cadherin in ten consecutive non-overlapping high power fields (HPF, 40× magnification). Counting was done for 14 days post UUO obstructed and unobstructed kidney sections from wild type and transgenic mice and was blinded with respect to treatment groups. The data reported are averages from four independent blinded counts.

Digital image analysis

Slides were quantitatively analyzed using the Nuance multispectral imaging system as previously described[33–35]. Spectral libraries were defined individually for each staining series as follows: trichrome (red and blue) and HSP27 (brown). Pixel counts and optical densities were determined after color separation was achieved using the defined spectral libraries. Five-non overlapping fields were scanned and analyzed for each kidney[33–35]. The pixel counts were normalized to the total image area.

Immunoblot analyses

Proteins were extracted from whole kidney tissue or NRK52E cell lysates as previously described (11). Protein lysates were separated by SDS-PAGE (10–20% resolving gel, Biorad, CA, cat. no. 161-1124), transferred to nitrocellulose membrane (Biorad, CA, cat. no. 161-0112) by `wet' electrophoretic transfer (80V for 1 hour), and blocked overnight at 4°C in 1% non-fat dry milk, 1% BSA, 0.05% Tween in PBS (Blotto B). Incubations with antibodies were at room temperature for 1 hour, except the antibodies for E-cadherin and β-catenin, which were incubated at 4°C overnight. For use, primary antibodies were diluted in Blotto B as follows: total HSP27 (Abcam, CA, cat. no. Ab8600, 1:1000), phosphorylated HSP27-S85 (Abcam, CA, cat. no. Ab5594, 1:4000), Phospho-p38MAPK (BD 612288, 1:500), HNE (Abcam, ab4654, 1:1000), α SMA (Sigma, St. Louis, MO, A2547, 1:2000), collagen III (Ab6310, Novus Biologicals, Littleton, CO, 1:100), E-cadherin (BD Biosciences, MD, cat. no. 610182) 1:100, β-catenin (BD Biosciences, MD, cat. no. 610153) 1:500, GAPDH (Abcam, CA, cat. no. ab8245) 1:500. HRP-conjugated goat anti-mouse (BD Transduction, MD, cat no. M15345) and goat anti-rabbit (eBiosciences, CA, cat. no. 18-8816-31) secondary antibodies were diluted in 10% non-fat dry milk, 0.1%BSA, 0.05% Tween in PBS at dilutions of 1:4500 and 1:10,000, respectively. HRP signals were visualized by enhanced chemiluminescence using a West Femto kit (Pierce, IL, cat. no. 34095) and recorded with a Fotodyne bench top CCD camera system. Densitometric quantification of immunoblot signals was done using Image J (NIH, rsbweb.nih.gov/ij/).

Statistical analyses

Continuous and categorical data were compared using non-parametric Mann-Whitney and Fisher's exact tests respectively. A p value ≤ 0.05 was considered significant.

Acknowledgments

This study was supported by the National Institutes of Health (grant NIDDK DK067981 5).

Grants and sources of support: Supported by the National Institutes of Health (NIDDK-DK067981-5)

References

1. Zeisberg M, Neilson EG. Mechanisms of Tubulointerstitial Fibrosis. J Am Soc Nephrol. 2010
2. Kalluri R. EMT: when epithelial cells decide to become mesenchymal-like cells. J Clin Invest. 2009; 119:1417–1419. [PubMed: 19487817]
3. Kalluri R, Weinberg RA. The basics of epithelial-mesenchymal transition. J Clin Invest. 2009; 119:1420–1428. [PubMed: 19487818]
4. Djamali A, Samaniego M. Fibrogenesis in kidney transplantation: potential targets for prevention and therapy. Transplantation. 2009; 88:1149–1156. [PubMed: 19935366]
5. Bedi S, Vidyasagar A, Djamali A. Epithelial-to-mesenchymal transition and chronic allograft tubulointerstitial fibrosis. Transplantation Reviews. 2008; 22:1–5. [PubMed: 18631853]
6. Iwano M, Plieth D, Danoff TM, et al. Evidence that fibroblasts derive from epithelium during tissue fibrosis. JClinInvest. 2002; 110:341–350.
7. Humphreys BD, Lin SL, Kobayashi A, et al. Fate tracing reveals the pericyte and not epithelial origin of myofibroblasts in kidney fibrosis. The American journal of pathology. 2010; 176:85–97. [PubMed: 20008127]
8. Kostenko S, Moens U. Heat shock protein 27 phosphorylation: kinases, phosphatases, functions and pathology. Cell Mol Life Sci. 2009
9. Huot J, Houle F, Spitz DR, et al. HSP27 phosphorylation-mediated resistance against actin fragmentation and cell death induced by oxidative stress. Cancer Res. 1996; 56:273–279. [PubMed: 8542580]
10. Guay J, Lambert H, Gingras Breton G, et al. Regulation of actin filament dynamics by p38 map kinase-mediated phosphorylation of heat shock protein 27. J Cell Sci. 1997; 110:357–368. [PubMed: 9057088]
11. Charette SJ, Lavoie JN, Lambert H, et al. Inhibition of Daxx-mediated apoptosis by heat shock protein 27. MolCell Biol. 2000; 20:7602–7612.
12. Havasi A, Wang Z, Gall JM, et al. Hsp27 inhibits sublethal, Src mediated renal epithelial cell injury. Am J Physiol Renal Physiol. 2009; 297:F760–768. [PubMed: 19553351]
13. Arrigo AP, Firdaus WJ, Mellier G, et al. Cytotoxic effects induced by oxidative stress in cultured mammalian cells and protection provided by Hsp27 expression. Methods. 2005; 35:126–138. [PubMed: 15649839]
14. Mairesse N, Bernaert D, Del Bino G, et al. Expression of HSP27 results in increased sensitivity to tumor necrosis factor, etoposide, and H2O2 in an oxidative stress-resistant cell line. J Cell Physiol. 1998; 177:606–617. [PubMed: 10092213]
15. Lambert H, Charette SJ, Bernier AF, et al. HSP27 multimerization mediated by phosphorylation-sensitive intermolecular interactions at the amino terminus. JBiolChem. 1999; 274:9378–9385.
16. Chevalier RL. Obstructive nephropathy: towards biomarker discovery and gene therapy. NatClinPractNephrol. 2006; 2:157–168.
17. Rhyu DY, Yang Y, Ha H, et al. Role of reactive oxygen species in TGF-beta1-induced mitogen-activated protein kinase activation and epithelial-mesenchymal transition in renal tubular epithelial cells. J Am SocNephrol. 2005; 16:667–675.
18. Vidyasagar A, Reese S, Acun Z, et al. HSP27 is involved in the pathogenesis of kidney tubulointerstitial fibrosis. Am J Physiol Renal Physiol. 2008; 295:F707–716. [PubMed: 18596079]
19. Djamali A, Reese S, Oberley T, et al. Heat shock protein 27 in chronic allograft nephropathy: a local stress response. Transplantation. 2005; 79:1645–1657. [PubMed: 15973165]
20. Bianco RA, Keen HL, Lavoie JL, et al. Untraditional methods for targeting the kidney in transgenic mice. American journal of physiology Renal physiology. 2003; 285:F1027–1033. [PubMed: 14600026]

21. Rogalla T, Ehrnsperger M, Preville X, et al. Regulation of Hsp27 oligomerization, chaperone function, and protective activity against oxidative stress/tumor necrosis factor alpha by phosphorylation. JBiolChem. 1999; 274:18947–18956.
22. Arrigo AP, Virot S, Chaufour S, et al. Hsp27 consolidates intracellular redox homeostasis by upholding glutathione in its reduced form and by decreasing iron intracellular levels. AntioxidRedoxSignal. 2005; 7:414–422.
23. Chen SW, Kim M, Song JH, et al. Mice that overexpress human heat shock protein 27 have increased renal injury following ischemia reperfusion. Kidney Int. 2009; 75:499–510. [PubMed: 19020532]
24. Kim M, Park SW, Chen SW, et al. Selective Renal Over-Expression of Human Heat Shock Protein 27 Reduces Renal Ischemia-Reperfusion Injury in Mice. Am J Physiol Renal Physiol. 2010
25. Stetler RA, Cao G, Gao Y, et al. Hsp27 protects against ischemic brain injury via attenuation of a novel stress-response cascade upstream of mitochondrial cell death signaling. The Journal of neuroscience : the official journal of the Society for Neuroscience. 2008; 28:13038–13055. [PubMed: 19052195]
26. Stetler RA, Gao Y, Signore AP, et al. HSP27: mechanisms of cellular protection against neuronal injury. Curr Mol Med. 2009; 9:863–872. [PubMed: 19860665]
27. Yamada S, Pokutta S, Drees F, et al. Deconstructing the cadherin-catenin-actin complex. Cell. 2005; 123:889–901. [PubMed: 16325582]
28. Kobielak A, Fuchs E. Alpha catenin: at the junction of intercellular adhesion and actin dynamics. Nat Rev Mol Cell Biol. 2004; 5:614–625. [PubMed: 15366705]
29. Bryant DM, Stow JL. The ins and outs of E-cadherin trafficking. Trends Cell Biol. 2004; 14:427–434. [PubMed: 15308209]
30. Lavoie JN, Lambert H, Hickey E, et al. Modulation of cellular thermoresistance and actin filament stability accompanies phosphorylation-induced changes in the oligomeric structure of heat shock protein 27. MolCell Biol. 1995; 15:505–516.
31. Berkowitz P, Hu P, Liu Z, et al. Desmosome signaling. Inhibition of p38MAPK prevents pemphigus vulgaris IgG-induced cytoskeleton reorganization. J BiolChem. 2005; 280:23778–23784.
32. Fanelli MA, Montt Guevara M, Diblasi AM, et al. P-Cadherin and beta-catenin are useful prognostic markers in breast cancer patients; beta catenin interacts with heat shock protein Hsp27. Cell Stress Chaperones. 2008
33. Levenson RM. Spectral imaging perspective on cytomics. Cytometry A. 2006; 69:592–600. [PubMed: 16680703]
34. Rojo MG, Bueno G, Slodkowska J. Review of imaging solutions for integrated quantitative immunohistochemistry in the Pathology daily practice. Folia histochemica et cytobiologica / Polish Academy of Sciences, Polish Histochemical and Cytochemical Society. 2009; 47:349–354.
35. Djamali A, Reese S, Hafez O, et al. Nox2 is a Mediator of Chronic CsA Nephrotoxicity. American journal of transplantation : official journal of the American Society of Transplantation and the American Society of Transplant Surgeons. 2012

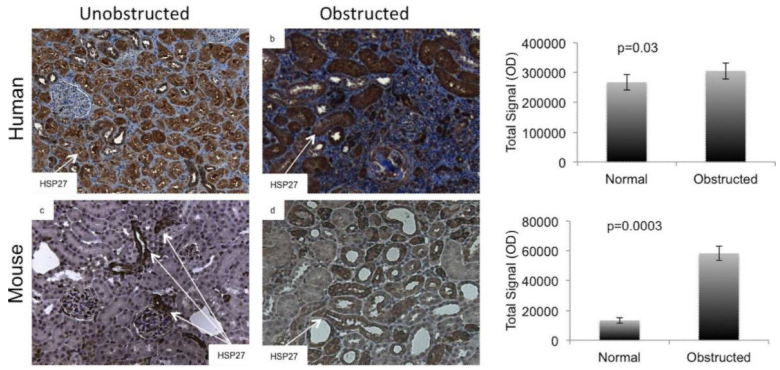

Fig. 1. Hsp27 was increased in tubules of human and mouse kidneys with obstruction

Tissue sections prepared from obstructed and unobstructed human and mouse kidneys (n=5 each group) were stained for HSP27 (dark brown). Digital image analyses using the Nuance multispectral imaging system showed that obstructed kidneys exhibited significantly more intense HSP27 staining in renal tubules.

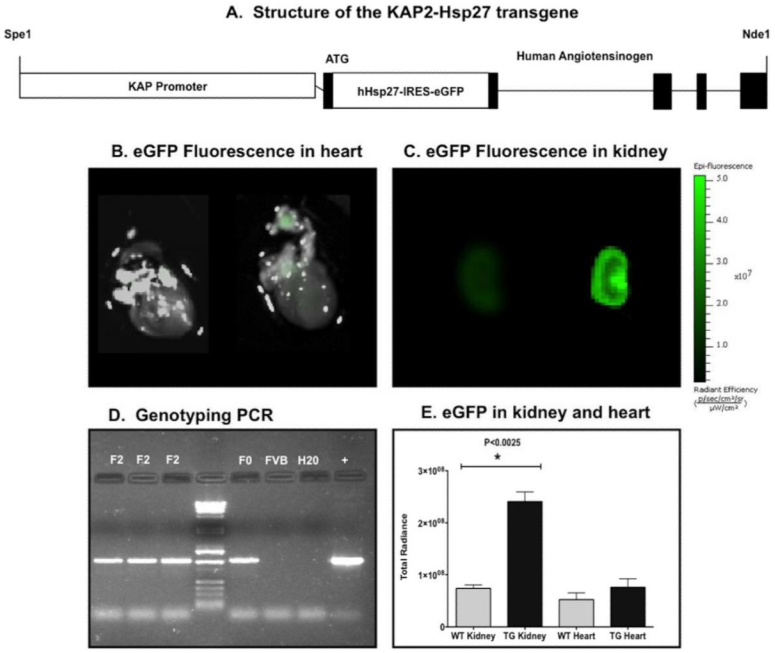

Fig. 2. Characterization of KAP2-HSP27 transgenic mice

(A) Schematic of the KAP2-HSP27 transgene. The protein coding region of the gene included the coding sequence for human HSP27 and an IRES-eGFP cassette so expression of the transgene coordinately produced both HSP27 and eGFP. (B, C, E) eGFP fluorescence was measured in hearts and kidneys from wild type (WT) or transgenic (TG) post pubescent male mice. Optimal excitation and emission wavelengths were 465 and 520 nm, respectively, using epi-illumination. The transgenic kidney (not the heart) showed greater fluorescence radiant efficiency than wild type. (D) PCR genotyping. The transgene PCR product was amplified with genomic DNA from three second-generation progeny (F2). Positive controls were amplifications with founder genomic DNA (F0) or with pKAP2-hHSP27 plasmid DNA (+). Negative controls were amplifications with wild type FVB DNA (FVB) and water (H2O).

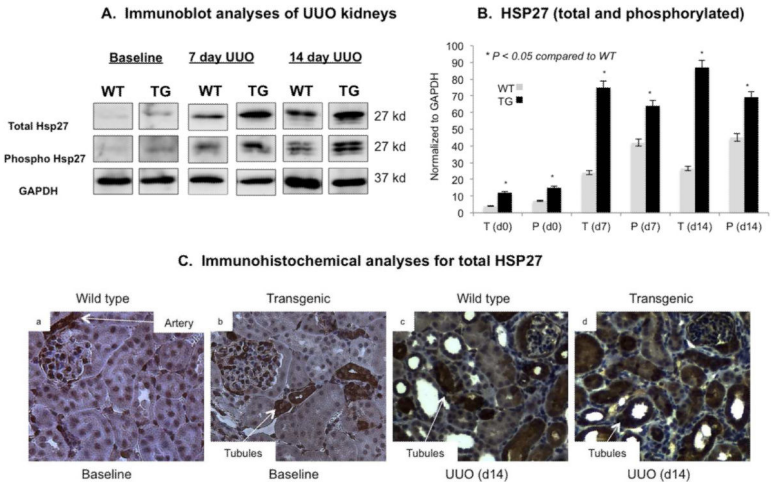

Fig. 3. HSP27 protein was increased at baseline and after UUO in transgenic mice

(A) Protein extracts from wild type (WT) and transgenic (TG) mice were analyzed by immunoblots at baseline, 7 and 14 days after UUO. (B) Immunoblots were quantitatively analyzed by Image J densitometry and values normalized to the corresponding GAPDH values. Total and phosphorylated-HSP27 levels were increased in transgenic mice compared to wild-type littermates (n=5 in each group). (C) Immunohistochemical analysis confirmed elevated tubular HSP27 in the transgenic mice at both baseline and after obstruction (only 14-day data shown).

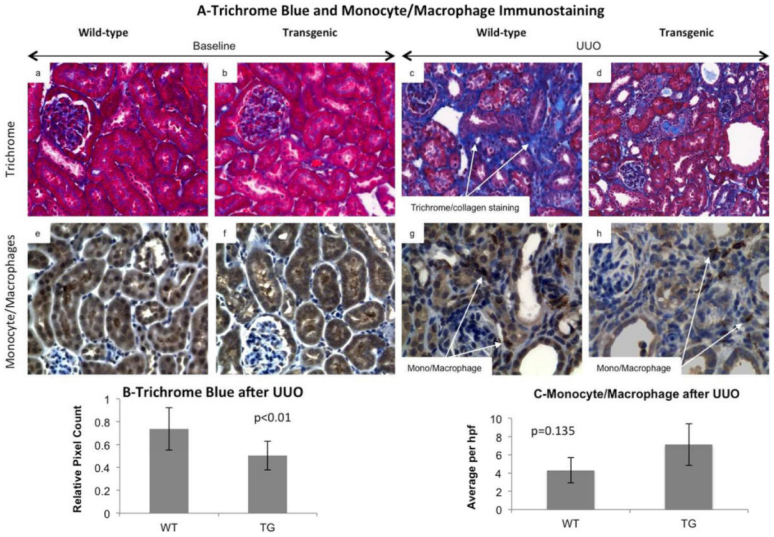

Fig. 4. Hsp27 overexpression was associated with decreased fibrosis after UUO

Tissue sections prepared from baseline and 14 day UUO kidneys from wild type and KAP-HSP27 transgenic mice were stained with trichrome aniline blue (A panels a–d) and quantitatively analyzed using the Nuance digital analysis software system (B). Trichrome blue staining was significantly reduced in the transgenic obstructed mice as compared to wild type mice ($p<0.01$). The data shown are representative of the group averages ($n=5$ in each group). Monocyte/macrophage infiltration was evaluated at baseline and after UUO in the cortex. While no infiltration was noted at baseline, both transgenic and wild type mice had increased staining following UUO. The difference between the 2 groups was not statistically significant.

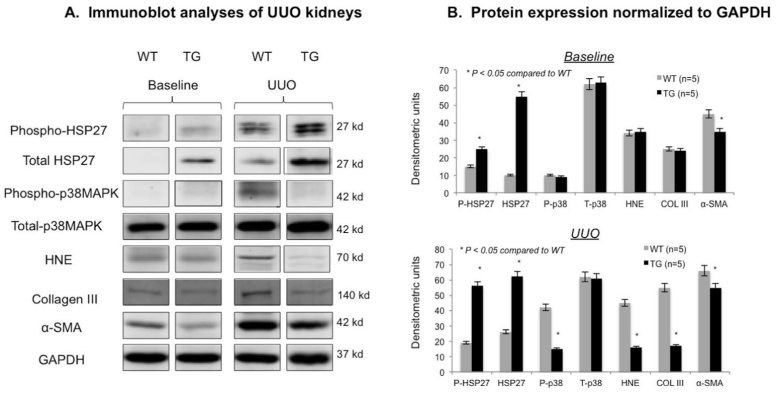

Fig. 5. HSP27 upregulation was associated with reduced fibrogenesis after UUO

(A) Immunoblot analyses for total and phosphorylated HSP27, total and phosphorylated p38MAPK, 4-Hydroxynonenal (HNE), collagen III, α-SMA and GAPDH on kidney extracts from wild type (WT) and transgenic (TG) mice at baseline and 14 days after UUO (n=5 in each group). (B) Immunoblots were quantitatively assessed by Image J and protein values were normalized to GAPDH. The studies showed that activated (phosphorylated) p38MAPK, collagen III, α-SMA and HNE were significantly decreased in obstructed transgenic kidneys compared to wild type. Total p38MAPK levels remained unchanged.

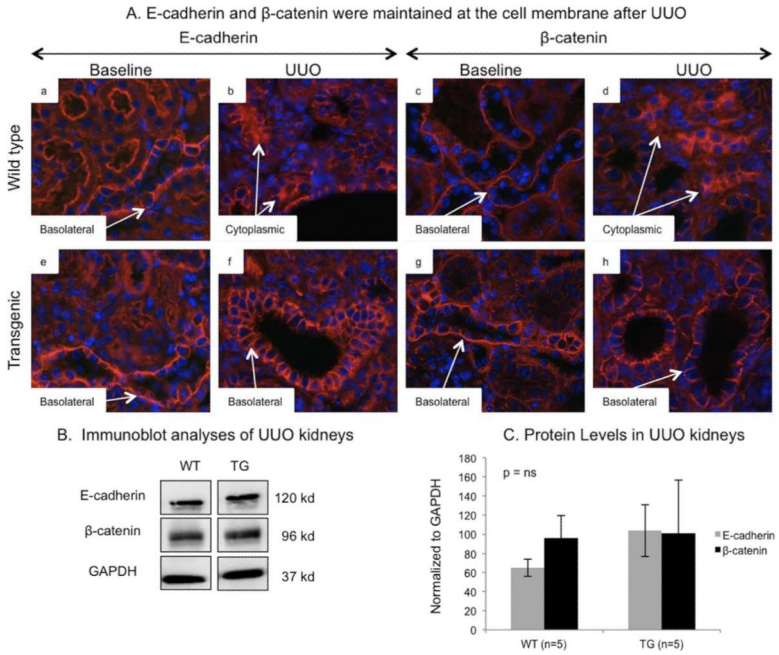

Figure 6. E-cadherin and β-catenin were maintained at the cell membrane in transgenic mice

Immunofluorescence studies for E-cadherin and β-catenin at baseline and day 14 after UUO in wild type and transgenic mice showed that tubular epithelial cells in wild type mice had greater cytoplasmic staining for E-cadherin and β-catenin after UUO (A, panels b and d). In contrast, tubular cells from transgenic mice retained E cadherin and β-catenin at the basolateral membranes (A, panels f and h). Immunoblot analyses demonstrated that E-cadherin and β-catenin levels remained unchanged after 14 days of UUO in wild type and transgenic mice (B and C, n=5 in each group).